The Mechanism of Adenosylmethionine-Dependent Activation of Methionine Synthase: A Rapid Kinetic Analysis of Intermediates in Reductive Methylation of Cob(II)alamin Enzyme †

ARTICLE *in* BIOCHEMISTRY · OCTOBER 1998

Impact Factor: 3.02 · DOI: 10.1021/bi9808565 · Source: PubMed

The Mechanism of Adenosylmethionine-Dependent Activation of Methionine Synthase: A Rapid Kinetic Analysis of Intermediates in Reductive Methylation of Cob(II)alamin Enzyme†

Joseph T. Jarrett,‡ David M. Hoover,§,||,⊥ Martha L. Ludwig,§,|| and Rowena G. Matthews*,§,||

Johnson Research Foundation and Department of Biochemistry and Biophysics, University of Pennsylvania, Philadelphia, Pennsylvania 19104, and Biophysics Research Division and Department of Biological Chemistry, University of Michigan, Ann Arbor, Michigan 48109

Received April 16, 1998; Revised Manuscript Received July 1, 1998

ABSTRACT: Cobalamin-dependent methionine synthase catalyzes the transfer of a methyl group from methyltetrahydrofolate to homocysteine, generating tetrahydrofolate and methionine. During this primary turnover cycle, the enzyme alternates between the active methylcobalamin and cob(I)alamin forms of the enzyme. Formation of the cob(II)alamin prosthetic group by oxidation of cob(I)alamin or photolysis of methylcobalamin renders the enzyme inactive. Methionine synthase from *E. coli* catalyzes its own reactivation by a reductive methylation that involves electron transfer from reduced flavodoxin and methyl transfer from AdoMet. This process has been proposed to involve formation of a transient cob(I)alamin intermediate that is then trapped by methyl transfer from AdoMet. During aerobic growth of *E. coli*, electrons for this process are ultimately derived from NADPH, and electron transfer does not generate a detectable level of cob(I)alamin due to the large potential difference between the NADPH/$NADP^+$ couple and the cob(I)alamin/cob(II)alamin couple. In this paper, we show that even in the presence of the strong reductant flavodoxin hydroquinone, cob(I)alamin is not observed as a significant intermediate. We demonstrate, however, that this is due to a rate-limiting reorganization of the cobalt ligand environment from five-coordinate to four-coordinate cob(II)alamin. Mutation of aspartate 757 to glutamate results in a cob(II)alamin enzyme that is ∼70% four-coordinate, and reductive methylation of this enzyme using flavodoxin hydroquinone as the electron donor proceeds through a kinetically competent cob(I)alamin intermediate. Furthermore, wild-type cob(I)alamin enzyme produced by chemical reduction reacts with AdoMet in a kinetically competent reaction. We provide evidence that methyl transfer from AdoMet to cob(I)alamin enzyme results initially in formation of a five-coordinate methylcobalamin enzyme that slowly decays to the active six-coordinate methylcobalamin enzyme. We propose a kinetic scheme for reductive methylation of wild-type cob(II)alamin enzyme by adenosylmethionine and flavodoxin hydroquinone in which slow conformational changes mask the relatively fast electron and methyl transfer steps.

Cobalamin-dependent methionine synthase from *E. coli* catalyzes the transfer of a methyl group from methylcobalamin enzyme to homocysteine, producing cob(I)alamin enzyme and methionine. The catalytic cycle is completed by the transfer of a methyl group from CH_3-H_4folate[1] to cob(I)alamin enzyme, generating H_4folate and regenerating the active methylcobalamin enzyme. Oxidation of cob(I)-alamin enzyme or photolysis of methylcobalamin enzyme leads to formation of inactive cob(II)alamin enzyme. In *E. coli*, methionine synthase catalyzes the reactivation of oxidized enzyme through a reductive methylation, in which electron transfer from reduced flavodoxin and methyl transfer from AdoMet lead to regeneration of the active methylcobalamin enzyme.

Since AdoMet was first reported to be essential for maintaining methionine synthase activity (*1*, *2*), a number of studies have examined enzyme activation and the role of AdoMet. Taylor and Weissbach first established that the methyl group from AdoMet is transferred to the cofactor, forming methylcobalamin enzyme (*3*), and that this activated methylcobalamin enzyme can undergo multiple turnovers with homocysteine and CH_3-H_4folate in the absence of AdoMet (*4*). A low-potential one-electron reducing system is also required for activity (*5*, *6*). This reducing system

† This research has been supported by NIH Research Grants GM24908 (R.G.M.) and GM16429 (M.L.L.). J.T.J. was supported in part by an NIH postdoctoral fellowship (GM17455).

* Correspondence should be addressed to this author at Biophysics Research Division, University of Michigan, 4024 Chemistry Building, 930 N. University Ave., Ann Arbor, MI 48109-1055.

‡ University of Pennsylvania.

§ Biophysics Research Division, University of Michigan.

|| Department of Biological Chemistry, University of Michigan.

⊥ Present address: National Cancer Institute, Frederick, MD 21702.

[1] Abbreviations: AdoHcy, *S*-adenosyl-L-homocysteine; AdoMet, *S*-adenosyl-L-methionine; EDTA, ethylenediaminetetraacetic acid; EPR, electron paramagnetic resonance; FAD, flavin adenine dinucleotide; Fld, flavodoxin; FMN, flavin mononucleotide; FNR, ferredoxin (flavodoxin):$NADP^+$ oxidoreductase; CH_3-H_4folate, 5-methyltetrahydrofolate; NADPH, nicotinamide adenine dinucleotide phosphate, reduced form; $NADP^+$, nicotinamide adenine dinucleotide phosphate; SHE, standard hydrogen electrode; H_4folate, 5,6,7,8-tetrahydrofolate; Tris, tris(hydroxymethyl)aminomethane hydrochloride.

S0006-2960(98)00856-3 CCC: $15.00
Published on Web 08/20/1998

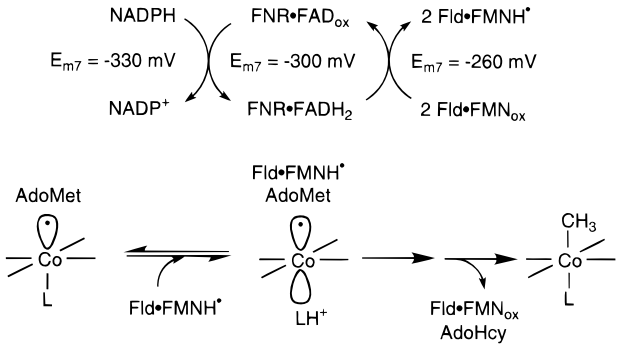

FIGURE 1: Scheme depicting the events leading to in vivo reductive methylation of cob(II)alamin enzyme. Under aerobic conditions, oxidized ferredoxin (flavodoxin):NADP^{+} oxidoreductase (FNR•FAD$_{ox}$) accepts a hydride from NADPH and transfers the electrons to flavodoxin (Fld•FMN$_{ox}$), generating primarily flavodoxin semiquinone. Under anaerobic conditions, the decarboxylation of pyruvate is coupled to reduction of flavodoxin, forming the flavodoxin hydroquinone as the major species. These reduced forms of flavodoxin bind to inactive cob(II)alamin enzyme, leading to a conformational change that is coupled with dissociation of His759 and protonation of the His759-Asp757-Ser810 triad (*15, 16, 22*). Electron transfer and methyl transfer result in formation of active methylcobalamin enzyme. Although NADPH oxidation ultimately produces 2 equiv of flavodoxin semiquinone, only one electron is transferred to methionine synthase during reductive methylation. Midpoint potentials cited are literature values (*11, 15, 30*).

was later shown to be involved in reductive methylation of oxidized enzyme (*7*), but is not required for anaerobic turnover of methylcobalamin enzyme with homocysteine and CH_3-H_4folate (*8, 9*). More recently it has been shown that electron transfer and methyl transfer are thermodynamically coupled reactions, and that the rate of formation of methylcobalamin enzyme is dependent on the degree of reduction of the oxidized enzyme (*10*). These experiments have led to a model for reductive methylation in which electron transfer leads to formation of a trace amount of cob(I)alamin enzyme, which is trapped by irreversible methyl transfer from AdoMet (*10*).

During aerobic growth, the electrons for reductive methylation are derived from NADPH via ferredoxin (flavodoxin): NADP^{+} oxidoreductase and flavodoxin [formerly referred to as the R and F proteins (*7, 11, 12, 13, 14*), Figure 1]. Under these conditions, electron transfer from reduced oxidoreductase to flavodoxin produces flavodoxin semiquinone as the major species. Since the flavodoxin semiquinone/oxidized midpoint potential [$E_{m7} = -260$ mV vs SHE (*15*)] is much higher than the cob(I)alamin/cob(II)alamin midpoint potential [$E_{m7} = -490$ mV (*16*)], the equilibrium does not favor cob(I)alamin formation, and it is not formed as a detectable intermediate following electron transfer from flavodoxin semiquinone to cob(II)alamin enzyme (*17*). In vitro, photochemical reduction of flavodoxin with deazaflavin and EDTA (*18*) allows conversion to the hydroquinone oxidation state. Since the flavodoxin hydroquinone/semiquinone couple [$E_{m7} = -440$ mV (*15*)] is close to the cob(I)alamin/cob(II)alamin couple, cob(I)alamin should be observed following electron transfer from flavodoxin hydroquinone to cob(II)alamin enzyme. Flavodoxin hydroquinone is also the major form of flavodoxin during anaerobic growth of *E. coli*, where it is produced by the action of a thiamine diphosphate-dependent pyruvate: flavodoxin oxidoreductase (*19*).

Recent studies have demonstrated that reorganization of the cobalt ligand environment and changes in the protein conformation are events that probably precede the electron and methyl group transfer steps that reactivate methionine synthase. The cobalt ligand environment in the wild-type cob(II)alamin enzyme is predominantly five-coordinate (*9*), with four equatorial nitrogen ligands provided by the corrin macrocycle and one axial nitrogen ligand provided by histidine 759 from the protein (*20, 21*). Reduction to the cob(I)alamin oxidation state is coupled to dissociation of His759 and protonation of the His759-Asp757-Ser810 hydrogen-bonded triad (*16*), resulting in formation of a four-coordinate cob(I)alamin cofactor. Flavodoxin binding favors reorganization of the five-coordinate cob(II)alamin enzyme to four-coordinate cob(II)alamin (*15*), an event that may prepare the cobalamin cofactor for electron transfer from the reduced flavin. Reorganization of the cobalt ligand environment appears to be coupled with a conformational change that alters the reactivity of the cob(I)alamin enzyme. Cob(I)alamin enzyme that is generated from methylcobalamin enzyme during primary turnover reacts rapidly with CH_3-H_4folate, but is much less reactive with AdoMet or flavodoxin, while cob(I)alamin enzyme that is generated by reduction is reactive with AdoMet and flavodoxin, but is unreactive with CH_3-H_4folate (*22*). These cob(I)alamin enzymes prepared by different routes also differ in their proteolytic fragmentation pathways when they are treated with trypsin (*22*). Together, these studies suggest that reductive methylation is associated with an altered conformation of the enzyme that is stabilized by flavodoxin binding.

In this paper, we demonstrate that reorganization of the cob(II)alamin ligand environment and/or the accompanying conformational change is the rate-limiting step in the overall reductive methylation pathway when flavodoxin hydroquinone is the electron donor. Bypassing this reorganization by mutation of Asp757 to glutamate allows observation of cob(I)alamin as a discrete intermediate. Cob(I)alamin enzyme, produced by the reaction of Asp757Glu cob(II)alamin enzyme with flavodoxin hydroquinone or by chemical reduction of wild-type cob(II)alamin enzyme (*22*), reacts rapidly with AdoMet. We use stopped-flow spectroscopy with a UV/visible diode-array detector to record absorption spectra of intermediates at intervals throughout these reactions, and are able to model the resulting spectra using previously reported spectra of the wild-type, Asp757Glu, and His759Gly enzymes (*21*). We further show that the immediate product of reductive methylation is an enzyme that has a spectrum similar to the methylcobalamin His759Gly enzyme, suggesting that the five-coordinate methylcobalamin cofactor is an intermediate in reductive methylation of wild-type enzyme. This five-coordinate methylcobalamin enzyme decays in a kinetically competent manner to the active six-coordinate methylcobalamin enzyme, a process that we propose is associated with conversion back to the active primary turnover conformation of the enzyme.

MATERIALS AND METHODS

Materials. Construction of the Asp757Glu mutation of methionine synthase and the methods for purification of overexpressed wild-type and mutant enzymes have been described (*23*). Wild-type methionine synthase was converted to the cob(II)alamin form by anaerobic treatment with

homocysteine and dithiothreitol, followed by gel filtration chromatography (*24*). Asp757Glu cob(II)alamin methionine synthase is easily oxidized in air; therefore, the enzyme was first converted to the methylcobalamin form by reductive methylation with AdoMet in an electrochemical cell (*24*). Immediately prior to use in stopped-flow experiments, the enzyme was equilibrated with an argon atmosphere and converted to cob(II)alamin enzyme by photolysis (described below). Flavodoxin was overexpressed and purified as previously described (*25*). The following were obtained from the indicated commercial sources and used without further purification: L-homocysteine thiolactone and *S*-adenosyl-L-methionine (iodide salt) from Sigma; methyl viologen and protocatechuic acid from Aldrich; (6*R*,*S*)-CH_3-H_4folate (calcium salt) from Schirks Laboratories. Titanium(III) citrate (80 mM) was prepared from titanium(III) chloride (1.9 M in 2 M HCl, Aldrich) as described previously (*24*, *26*). Phosphate buffer refers to potassium phosphate buffer at pH 7.2, unless otherwise specified.

For stopped-flow studies of reductive methylation, flavodoxin was reduced to the semiquinone or hydroquinone oxidation state by photoirradiation in the presence of deazaflavin and EDTA (*18*). Oxidized flavodoxin (150 μM) and 5-deazaflavin-3-sulfonate were mixed in 10 mM potassium phosphate buffer containing 0.5 mM EDTA, and placed in a glass tonometer along with protocatechuic acid (0.5 mM), while protocatechuate dioxygenase ($\sim$0.1 mg) was placed in a sidearm. Semiquinone flavodoxin was obtained using 1 μM deazaflavin, while hydroquinone flavodoxin was obtained using 10 μM deazaflavin. The tonometer was equilibrated with argon, and protocatechuate dioxygenase was mixed with the flavodoxin solution to remove residual oxygen. The tonometer was immersed in cold water and irradiated with a 600 W tungsten/halogen lamp through the side of the beaker. After three 10 s exposures, the semiquinone protein appears as a dark blue solution while the hydroquinone protein appears as a pale yellow solution. UV/visible spectra of each protein solution were used to estimate the relative concentrations of oxidized, semiquinone, and hydroquinone oxidation states.

To measure AdoMet-dependent reductive methylation, wild-type cob(II)alamin enzyme (30 μM) and AdoMet (200 μM) were mixed in 10 mM potassium phosphate buffer in a glass tonometer, and equilibrated with argon. To avoid rapid oxidation of Asp757Glu cob(II)alamin enzyme in air, this mutant enzyme was prepared as a solution of methylcobalamin enzyme (30 μM) and AdoMet (200 μM) in 10 mM potassium phosphate buffer in a glass tonometer. Following equilibration with argon, the enzyme was converted to the cob(II)alamin oxidation state by 5 s irradiation with a 600 W tungsten/halogen lamp as described above. To maintain anaerobiosis, all solutions were prepared with protocatechuic acid and protocatechuate dioxygenase as described above. The cob(II)alamin enzyme and AdoMet were rapidly mixed with reduced flavodoxin in an anaerobic stopped-flow spectrophotometer at 25 °C, and spectra were recorded at intervals from 2 ms to 10 s using a xenon lamp and a diode-array spectrophotometer. To minimize photoreduction of the deazaflavin and slow photolysis of the methylcobalamin product, a 360 nm cutoff filter was inserted in the light path immediately following the xenon lamp. Single-wavelength kinetic traces were also obtained using a tungsten lamp, a monochromator, and a photomultiplier tube.

The conversion of five-coordinate cob(II)alamin enzyme to four-coordinate cob(II)alamin enzyme accompanying flavodoxin binding was measured by rapidly mixing wild-type cob(II)alamin enzyme (30 μM) + AdoMet (200 μM) with oxidized flavodoxin (150 μM), both in 10 mM potassium phosphate buffer, pH 7.2, in a stopped-flow spectrophotometer at 25 °C. Spectra were measured before and after the reaction, and spectral changes were followed at 465 and 477 nm. The methylation of cob(I)alamin methionine synthase by AdoMet was observed by reducing the wild-type enzyme with titanium(III) citrate (*24*). Wild-type cob(II)alamin enzyme (30 μM) in 10 mM Tris, pH 7.2, was placed in a tonometer and equilibrated with argon. Titanium(III) citrate (4 mM) was added with a syringe and the enzyme equilibrated for 10 min, producing enzyme that contains $\sim$70−80% cob(I)alamin and $\sim$20−30% cob(II)alamin cofactor. This enzyme mixture was rapidly mixed in a stopped-flow spectrophotometer with AdoMet (200 μM) at 25 °C, and spectra were recorded from 2 ms to 1 s using the diode-array configuration described above. Single-wavelength traces were obtained at selected wavelengths to monitor the formation and decay of transient intermediates.

RESULTS

A Scheme for the Participation of Cob(I)alamin as an Intermediate in Reductive Methylation. Reductive methylation of wild-type cob(II)alamin methionine synthase is accomplished via electron transfer from reduced flavodoxin and methyl transfer from AdoMet; presumably both transfers directly involve the cobalamin cofactor. Electron transfer to the five-coordinate cob(II)alamin cofactor would generate cob(I)alamin as an intermediate and require prior or concomitant dissociation of His759 from the cobalt, while methyl transfer to this cob(I)alamin intermediate must regenerate the resting six-coordinate methylcobalamin enzyme, and therefore requires recoordination of His759 to the cobalt. Based on these necessary chemical events, a scheme is proposed for changes in the cobalamin oxidation state and coordination environment that lead from five-coordinate cob(II)alamin to six-coordinate methylcobalamin enzyme (Figure 2, top). Each of these proposed species has been generated by chemical treatment of the wild-type enzyme or by mutagenesis, and each has a unique UV/visible spectrum (Figure 2). These unique spectra in principle allow direct observation of each species as a transient intermediate using stopped-flow UV/visible spectroscopy. Unfortunately, the observations are complicated by temporal overlap of the kinetic phases, and transient changes in the spectra of the enzyme during reductive methylation often arise from mixtures of the intermediate species. To analyze the experiments described below, we have estimated rate constants by fitting single-wavelength transient absorbance changes, including those shown in Figures 4−7, to multiple exponential functions. These rate constants were then substituted into the various kinetic steps in Figure 2, and HopKINSIM kinetic modeling software (D. Wachsstock, Johns Hopkins University) was used to simulate transient changes in the concentrations of each intermediate (data not shown). We were then able to model the transient absorbance changes using known extinction coefficients for each

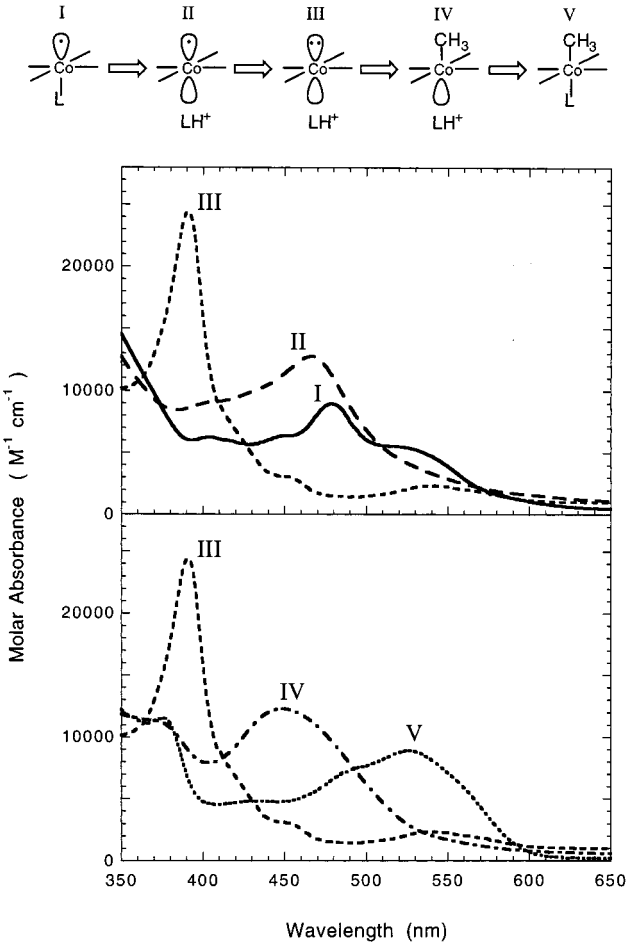

FIGURE 2: General scheme for the sequence of reactions and intermediates in reductive methylation is shown at the top of the figure. Five-coordinate cob(II)alamin enzyme (I) is converted to four-coordinate cob(II)alamin enzyme (II) by dissociation and protonation of the lower axial ligand, and then reduced to cob(I)alamin (III) by electron transfer from flavodoxin or chemical reductants. Methyl transfer from AdoMet to cob(I)alamin enzyme (III) generates five-coordinate methylcobalamin enzyme (IV), which is then converted to the stable six-coordinate methylcobalamin enzyme (V) by recoordination of the lower axial ligand. Upper panel: five-coordinate cob(II)alamin (I, —), four-coordinate cob(II)alamin (II, — —), and cob(I)alamin (III, - - -). Lower panel: cob(I)alamin (III, - - -), five-coordinate methylcobalamin (IV, — • —), and six-coordinate methylcobalamin (V, ···). Spectra of four-coordinate cob(II)alamin and five-coordinate methylcobalamin are based on experimentally determined spectra of the His759Gly mutant enzyme. Spectra of cob(I)alamin and six-coordinate methylcobalamin enzyme are those measured for wild-type enzyme. The five-coordinate cob(II)alamin spectrum is calculated from the wild-type spectrum assuming the wild-type enzyme is a mixture of 85% five-coordinate and 15% four-coordinate cob(II)alamin enzyme.

of the intermediate species. Using these modeled data, we have predicted spectra of the enzyme mixtures at various times throughout reductive methylation and compared the predicted spectra to spectra recorded with a stopped-flow diode-array spectrophotometer. Successive iterations of this process have developed a self-consistent kinetic and spectral interpretation of the experiments described below.

The Rate of Reductive Methylation of Cob(II)alamin Enzyme Is Partially Limited by the Reduction Potential of the in Vivo Reducing System. In vivo reducing systems that provide electrons for reductive methylation of cob(II)alamin methionine synthase in *E. coli* include NADPH and ferredoxin (flavodoxin):$NADP^+$ oxidoreductase (*7*), yielding flavodoxin in the semiquinone oxidation state, and pyruvate and pyruvate:flavodoxin oxidoreductase, yielding flavodoxin in the hydroquinone oxidation state (*19*). Figure 3 compares the rate of reduction of enzyme in the cob(II)alamin form in the presence of AdoMet and an excess of either the flavodoxin semiquinone or the hydroquinone. We have assumed that the 75 μM concentration of reduced flavodoxin is sufficient to saturate methionine synthase (*15*), although this has not been rigorously tested. In the presence of flavodoxin semiquinone, cob(II)alamin enzyme is cleanly converted to methylcobalamin with an apparent rate constant of 0.01 s^{-1} at 25 ° C (Figure 3, squares). In the presence of flavodoxin hydroquinone, the rate of reductive methylation was increased considerably relative to rates with flavodoxin semiquinone as donor. However, the formation of methylcobalamin enzyme is kinetically complex when flavodoxin hydroquinone is the electron donor (Figure 3, diamonds); to allow comparison to the reaction with flavodoxin semiquinone (squares), we have used changes in absorbance at 525 nm as a crude measure of the rate of methylcobalamin formation. Based on these data, the half-time for formation of methylcobalamin enzyme is estimated to be ~1.2 s, indicating an approximately 50-fold increase in the rate of methylation as compared to the reaction with flavodoxin semiquinone. Since the primary difference between these experiments is the redox state of flavodoxin, the rate of reductive methylation with flavodoxin semiquinone as electron donor must be at least partially limited by the relatively high midpoint potential of the flavodoxin semiquinone/oxidized couple. The poor reducing power of

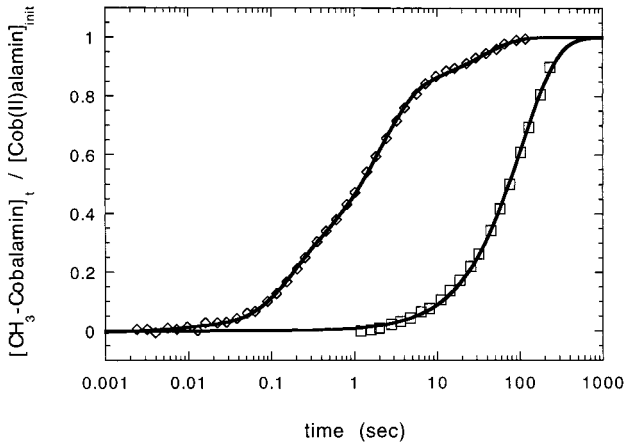

FIGURE 3: Reductive methylation of cob(II)alamin enzyme with AdoMet and reduced flavodoxin. Reductive methylation of methionine synthase in the cob(II)alamin form with flavodoxin semiquinone (□): 30 μM enzyme and 200 μM AdoMet were mixed with 150 μM flavodoxin semiquinone in a stopped-flow spectrophotometer, and the reaction was monitored at 525 nm. The reaction proceeds with an apparent rate constant of 0.01 s^{-1} at 25 °C. Reductive methylation of methionine synthase with flavodoxin hydroquinone (◇): 30 μM enzyme and 200 μM AdoMet were mixed with 150 μM flavodoxin hydroquinone in a stopped-flow spectrophotometer, and the reaction was monitored at several wavelengths (525 nm trace shown here). Although the reaction is multiphasic, a rough estimate of the rate constant can be calculated from the half-time of ~1.2 s at 25 °C; reductive methylation proceeds approximately 50-fold faster in the presence of flavodoxin hydroquinone than in the presence of an equal concentration of flavodoxin semiquinone. The solid curve is fit to a five-exponential function using a Marquardt−Levenberg algorithm while holding fixed the four rate constants determined from the data in Figure 4.

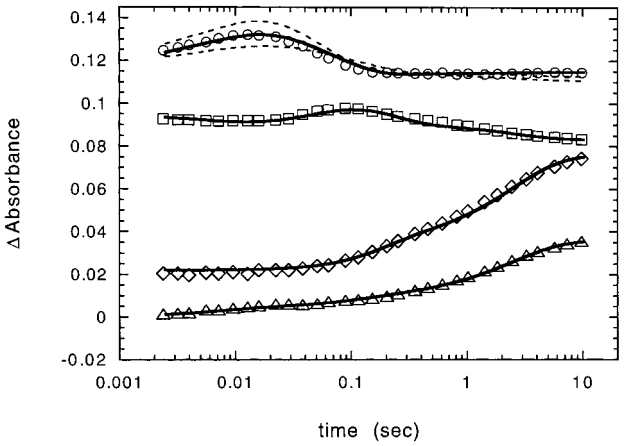

FIGURE 4: Spectral changes observed during reductive methylation of cob(II)alamin enzyme by excess AdoMet and flavodoxin hydroquinone suggest that early intermediates are formed during reductive methylation. Experimental conditions are the same as in Figure 3 (◇). An initial increase in absorbance at 390 nm (○) and 580 nm (△) suggests that electron transfer from flavodoxin hydroquinone to cob(II)alamin ($k_{obs} = 130\ s^{-1}$) leads to formation of cob(I)alamin and flavodoxin semiquinone, reaching a maximum concentration of ~0.5 ± 0.2 μM cob(I)alamin at 11 ms. The absorbance at 390 nm dissipates and the absorbance of the mixture increases at 450 nm (□, $k_{obs} = 25\ s^{-1}$), while spectral changes are not initially observed at 525 nm (◇). This suggests that an intermediate is formed at ~80 ms with a maximal absorbance at ~450 nm prior to the formation of significant amounts of six-coordinate methylcobalamin enzyme. Formation of active methylcobalamin enzyme is then observed at 525 nm (◇) and proceeds in two phases with apparent rate constants of 10 and 0.5 s^{-1}. In each case, the solid curve is a simulation using the spectra in Figure 2 and the kinetic scheme depicted in Figure 8. For 390 nm data (circles), the solid curve is simulated with $\Delta E_m = -4$ mV for electron transfer, while the dashed curves indicate simulations with $\Delta E_m = -20$ mV (upper curve) and +20 mV (lower curve). Kinetic traces have been shifted along the vertical axis to allow easier comparison.

flavodoxin semiquinone may result in a decrease in the electron transfer rate and/or the resulting cob(I)alamin population; both of these effects would decrease the overall rate of reductive methylation.

When the reaction of cob(II)alamin enzyme with AdoMet and flavodoxin hydroquinone was monitored at several wavelengths, it appeared that the enzyme was methylated in at least three separate stages (Figures 3 and 4). Initially, over the time range from 0.001 to 0.5 s, a small rapid increase in absorbance at 390 nm suggests that ~10% of the enzyme is reduced to cob(I)alamin with an apparent rate constant of 130 s^{-1} (Figure 4, circles). The absorbance at 390 nm then decreases with a rate constant of 25 s^{-1} (circles), and the absorbance at 450 nm increases at 25 s^{-1} (Figure 4, squares). The absorbance at 450 nm then falls at 10 s^{-1} (squares), while the absorbance at 525 nm (Figure 4, diamonds) increases with the same rate constant. On a somewhat slower time scale (0.5−10 s), the continued increase in absorbance at 525 nm suggests that ~80% of the enzyme is converted directly from cob(II)alamin to methylcobalamin with an apparent rate constant of ~0.5 s^{-1} (Figure 4, diamonds). Finally, on a much slower time scale (10−200 s), ~10% of the enzyme is converted from cob(II)alamin to methylcobalamin with an apparent rate constant of 0.02 s^{-1} (Figure 3, diamonds). We are unable to model this final very slow phase of methylation, which may be a reaction of damaged enzyme, and it has been ignored in Figure 4 and subsequent data analyses. The ratio of the amplitudes of the fast (0.001−0.5 s) methylation reactions to the slower (0.5−10 s) reaction (~1:8) is similar to the ratio of four-coordinate to five-coordinate cob(II)alamin that was observed for the wild-type enzyme by EPR spectroscopy (*21*), suggesting that dissociation of His759 from the cob(II)alamin cofactor may be limiting the rate of the slow phase of reductive methylation.

Dissociation of His759 from the Cobalt Is Rate-Limiting in the Conversion of Cob(II)alamin Enzyme to Methylcobalamin Enzyme. Using EPR and UV/visible spectroscopy, we have previously shown that flavodoxin binding to cob(II)alamin methionine synthase results in dissociation of His759 from the cobalt (*15*). This results in a shift in the principle visible absorption band from 477 to 465 nm and an increase in the extinction coefficient from 9470 to 12 500 $M^{-1}\ cm^{-1}$ (*21*). We rapidly mixed oxidized flavodoxin with wild-type cob(II)alamin in the stopped-flow spectrophotometer and were able to use this spectral shift to detect formation of the four-coordinate cob(II)alamin enzyme. We found that dissociation of His759 from the cobalt occurs at approximately the same rate as the slow phase for reductive methylation of wild-type enzyme ($k_{obs} = 0.4\ s^{-1}$, Figure 5, solid curve), suggesting that this event is rate-limiting in the reductive methylation of five-coordinate cob(II)alamin enzyme. To verify that the spectral changes seen were due to dissociation of His759 from the cobalt, spectra of the enzyme solutions prior to mixing and after 80 s were used to calculate a difference spectrum for the complete reaction (Figure 5, inset). This difference spectrum was compared with one calculated using the spectra of wild-type and His759Gly cob(II)alamin enzymes (*21*). Differences between the predicted and measured difference spectra from 480 to 550 nm may indicate that the His759Gly mutant is not a perfect model for wild-type four-coordinate cob(II)alamin enzyme.

The Asp757Glu Mutant Enzyme Contains Four-Coordinate Cob(II)alamin and Allows Direct Observation of the Electron and Methyl Transfer Reactions. Mutation of Asp757 to Glu results in a cob(II)alamin enzyme that contains ~70% four-coordinate and ~30% five-coordinate cob(II)alamin (*21*). If dissociation of His759 from the cobalt is rate-limiting in reductive methylation, the four-coordinate cob(II)alamin enzyme should be completely methylated at a rate that is comparable to the fast phase observed for wild-type enzyme, and cob(I)alamin enzyme should be observed as a discrete intermediate. We mixed Asp757Glu cob(II)alamin enzyme and AdoMet with flavodoxin hydroquinone, and observed an increase in absorbance at 390 and 580 nm that suggested electron transfer from flavodoxin hydroquinone to cob(II)alamin, forming cob(I)alamin enzyme and flavodoxin semiquinone with an apparent rate constant of 130 s^{-1} (Figure 6A). Since initial changes in absorbance at 390 nm are primarily due to cob(I)alamin formation and changes in absorbance at 580 nm are primarily due to flavodoxin semiquinone formation, we used known extinction coefficients for these enzyme forms to calculate the stoichiometry of product formation during electron transfer (Figure 6B). The initial rise in absorbance at 390 and 580 nm corresponded to approximately stoichiometric cob(I)alamin (4.7 μM at 15 ms) and flavodoxin semiquinone (4.2 μM at 15 ms) formation. The absorbance at 390 nm subsequently falls,

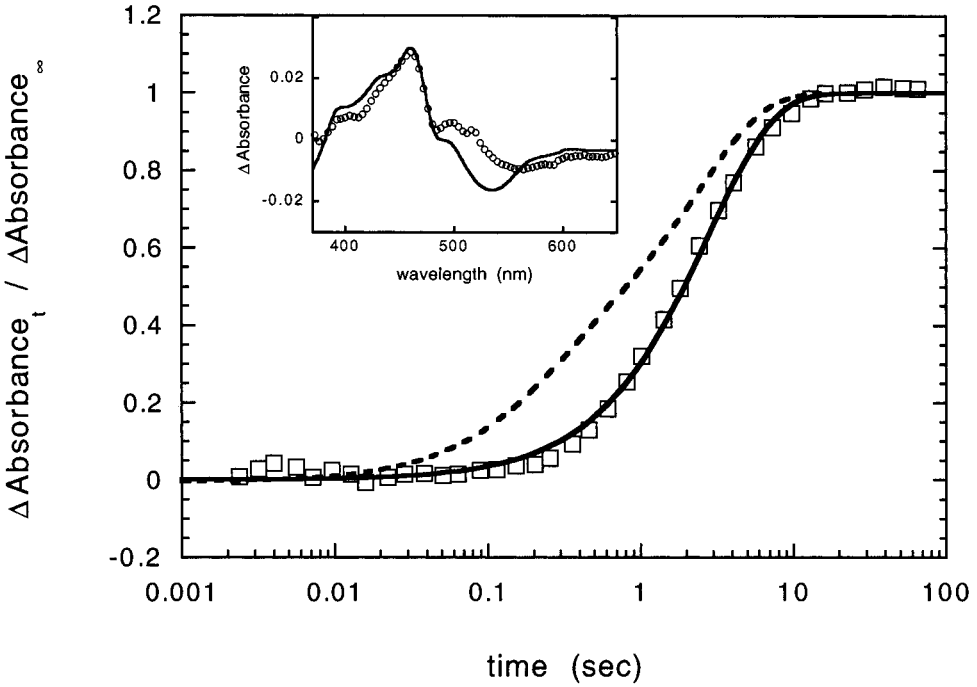

FIGURE 5: Conversion of wild-type five-coordinate cob(II)alamin enzyme to four-coordinate cob(II)alamin enzyme. Wild-type cob(II)alamin enzyme (15 μM) and AdoMet (200 μM) were mixed with oxidized flavodoxin (150 μM), and spectral changes were monitored at 465 nm (□). The rate of His759 dissociation ($k_{obs} = 0.4$ s^{-1}, solid curve) is compared to reductive methylation catalyzed by excess flavodoxin hydroquinone as assessed from the ΔA_{525} trace in Figure 4 (dashed curve). The changes in the spectrum of the cob(II)alamin enzyme:flavodoxin mixture (inset, ○) are modeled using spectra of the wild-type and His759Gly cob(II)alamin enzyme [solid curve (*21*)], suggesting that the observed spectral changes correspond to dissociation of His759 from the cobalt. The rate of His759 dissociation and the rate of the slowest phase of reductive methylation (over the range 2−10 s) are fit with similar rate constants (0.4 and 0.5 s^{-1}, respectively), suggesting that dissociation of His759 and accompanying conformational changes (*22*) may be largely rate-limiting in reductive methylation with AdoMet and flavodoxin hydroquinone.

and the absorbance at 535 nm rises; these absorbance changes are biphasic and share apparent rate constants of 25 and 10 s^{-1} (Figure 6A). These spectral changes correspond to the conversion of cob(I)alamin enzyme to methylcobalamin enzyme; the source of two kinetic rate constants becomes apparent in experiments described below.

To characterize the intermediates formed during reductive methylation of the Asp757Glu enzyme, we modeled the spectra obtained at intervals throughout the reaction, using the previously reported spectra of the Asp757Glu and His759Gly mutant enzymes and the known spectra of flavodoxin hydroquinone and semiquinone. The ratios of components in mixtures of intermediates were predicted using the kinetic model described in Figure 8 and HopKINSIM kinetic modeling software. A difference spectrum representing the initial phase of electron transfer was generated by subtracting spectra recorded at 10 and 2.6 ms (Figure 6C, upper panel), and is accurately modeled to conversion of 2.1 μM four-coordinate cob(II)alamin enzyme to 1.7 μM cob(I)alamin and 0.4 μM five-coordinate methylcobalamin enzyme, and conversion of 2.1 μM flavodoxin hydroquinone to semiquinone. A difference spectrum was also generated for the subsequent methylation of Asp757Glu cob(I)alamin enzyme by subtracting spectra recorded at 200 and 26 ms (Figure 6C, lower panel). This difference spectrum is somewhat more difficult to simulate due to the mixing of kinetic phases corresponding to methylation and to reduction of additional cob(II)alamin enzyme. The primary reaction modeled is the conversion of 3.3 μM four-coordinate cob(II)alamin enzyme and 2.4 μM cob(I)alamin enzyme to 1.3 μM five-coordinate and 4.7 μM six-coordinate methylcobalamin enzyme. These reactions are accompanied by conversion of an additional 3.3 μM flavodoxin hydroquinone to semiquinone.

As described in more detail for the wild-type enzyme (below), we have invoked a five-coordinate methylcobalamin enzyme as a transient intermediate in reductive methylation to account for the apparent biphasic kinetics observed for methylation of cob(I)alamin enzyme. The spectrum of His759Gly methylcobalamin enzyme [Figure 2 (*21*)] was used for accurate simulation of the observed difference spectra. The dashed curve in Figure 6C corresponds to a calculated spectrum assuming cob(I)alamin enzyme is converted directly to six-coordinate methylcobalamin enzyme, while the solid curve assumes initial formation of five-coordinate methylcobalamin enzyme at 25 s^{-1} followed by conversion to six-coordinate methylcobalamin enzyme at 10 s^{-1}.

Chemical Reduction of Wild-Type Enzyme to the Cob(I)alamin Form Allows Observation of Methyl Transfer and Recoordination of His759 to the Cobalt. Although the mutation of Asp757 to Glu allowed observation of intermediates in reductive methylation, these experiments did not allow unambiguous identification of five-coordinate methylcobalamin cofactor as the immediate product of methyl transfer from AdoMet to the cob(I)alamin prosthetic group. Identification was complicated by overlap between changes in the flavodoxin spectrum and critical regions of the cobalamin spectrum. We were able to avoid this spectral interference by chemically reducing wild-type cob(II)alamin enzyme with titanium(III) citrate (*22, 26*). This chemical reduction resulted in formation of a mixture of ~8 μM cob-

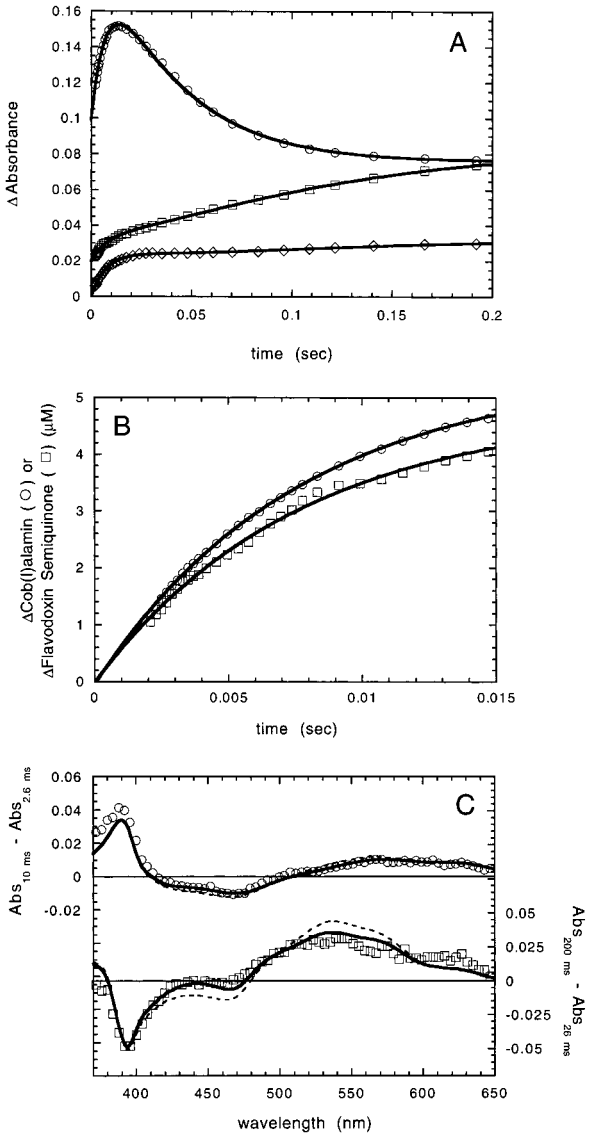

FIGURE 6: Reductive methylation of Asp757Glu cob(II)alamin enzyme confirms that cob(I)alamin is formed as a competent intermediate during reductive methylation. Asp757Glu cob(II)-alamin enzyme is ~70% four-coordinate cob(II)alamin, and this fraction of the enzyme can react with reduced flavodoxin without prior rate-limiting dissociation of His759 from the cobalt. Asp757Glu cob(II)alamin enzyme [20 μM total, ~14 μM four-coordinate cob(II)alamin] was rapidly mixed with AdoMet (100 μM) and flavodoxin hydroquinone (75 μM) in a stopped-flow spectrophotometer. (A) Changes in absorbance at 390 nm (○), 535 nm (□), and 580 nm (◇) are plotted vs time after mixing; curves have been shifted arbitrarily along the *y*-axis to allow easier comparison. (B) The initial changes in absorbance at 390 and 580 nm were used to calculate the concentration of cob(I)alamin and flavodoxin semiquinone over the first 15 ms using previously reported extinction coefficients (*15*, *16*). The similarity of these calculated curves suggests that electron transfer is approximately stoichiometric. Slight differences between these curves may be due to uncertainties in the extinction coefficients of the proteins involved. (C) Upper panel: spectral changes observed during the reduction of four-coordinate cob(II)alamin enzyme (○, 10 ms spectrum − 2.6 ms spectrum). Lower panel: spectral changes observed during methylation of cob(I)alamin enzyme (□, 200 ms spectrum − 26 ms spectrum). Solid curves are calculated from the model in Figure 8 and spectra in Figure 2 as described in the text. The dashed curves correspond to the spectra predicted by a model that does not include five-coordinate methylcobalamin enzyme.

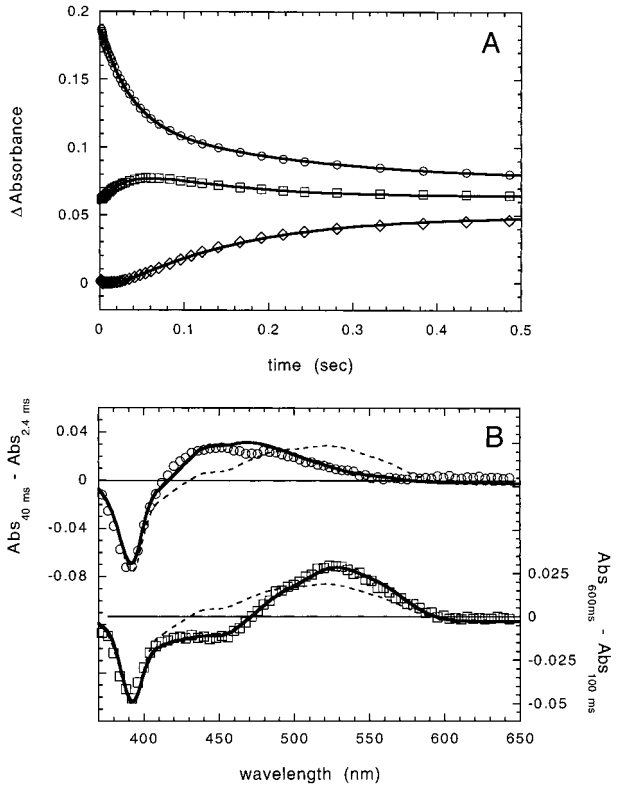

FIGURE 7: AdoMet methylation of wild-type cob(I)alamin enzyme. Wild-type cob(II)alamin enzyme (15 μM) was reduced with titanium(III) citrate, yielding a mixture of ~8−9 μM cob(I)alamin and ~6−7 μM cob(II)alamin enzyme, which was then rapidly mixed with AdoMet (100 μM) in a stopped-flow spectrophotometer. (A) Changes in absorbance at 390 (○), 450 (□), and 525 nm (◇) are plotted vs time after mixing. Curves have been shifted arbitrarily along the *y*-axis to allow easier comparison. (B) Upper panel: spectral changes observed during the methylation of cob(I)alamin enzyme to form five-coordinate methylcobalamin enzyme (○, 40 ms spectrum − 2.4 ms spectrum). Lower panel: spectral changes observed during conversion of five-coordinate methylcobalamin enzyme to six-coordinate methylcobalamin enzyme (□, 600 ms spectrum − 100 ms spectrum). Solid curves are calculated from the model in Figures 8 and spectra in Figure 2 as described in the text. The dashed curves correspond to the spectra predicted by a model that does not include five-coordinate methylcobalamin enzyme.

(I)alamin enzyme and ~7 μM cob(II)alamin enzyme, and this mixture was rapidly mixed with AdoMet in a stopped-flow spectrophotometer. A rapid decrease in absorbance at 390 nm (Figure 7A, circles) coincided with an increase in absorbance at 450 nm (squares), and both were associated with an apparent rate constant of 25 s^{-1}. The absorbance at 450 nm then dissipated, and the absorbance at 525 nm (diamonds) increased with an apparent rate constant of 10 s^{-1}. We used a diode-array detector to record spectra throughout the reaction, and have simulated the observed difference spectra using spectra of the wild-type cob(I)alamin and methylcobalamin enzymes and the His759Gly methylcobalamin enzyme (*21*). Again, the ratios of mixtures of intermediates were predicted using the kinetic model described in Figure 8 and HopKINSIM kinetic modeling software. A difference spectrum representing the initial disappearance of cob(I)alamin enzyme was generated by subtracting spectra recorded at 40 and 2.4 ms (Figure 7B, circles); this spectrum is modeled to conversion of 4.7 μM cob(I)alamin enzyme to 3.3 μM five-coordinate and 1.4 μM six-coordinate methylcobalamin enzyme (solid curve). A difference spectrum representing predominantly the final

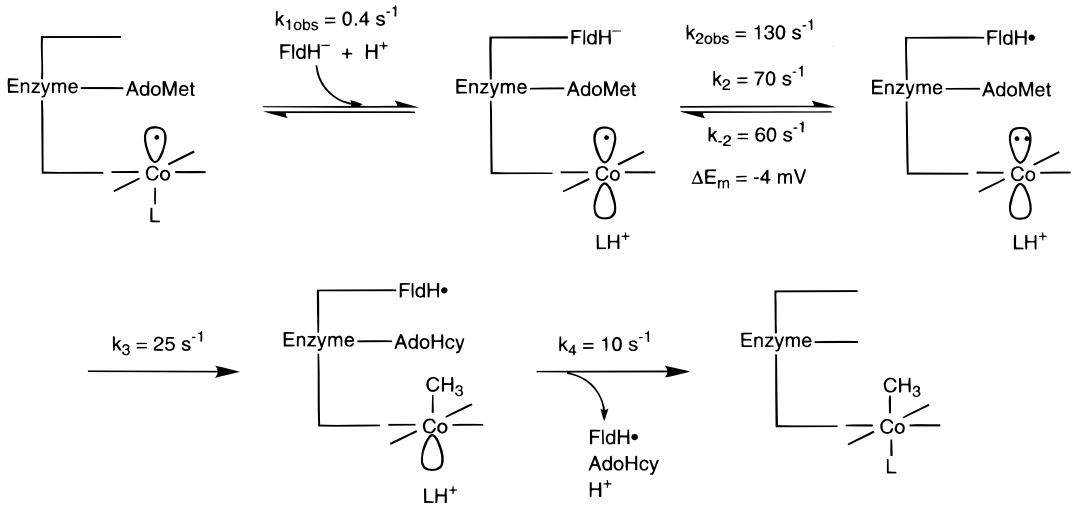

FIGURE 8: Kinetic model used to simulate steps in the reductive methylation of wild-type and Asp757Glu cob(II)alamin enzyme. The inactive cob(II)alamin enzyme contains tightly bound AdoMet and is an equilibrium mixture of five-coordinate and four-coordinate cob(II)alamin forms (*21*). Flavodoxin binding is coupled to proton uptake and conversion to the four-coordinate cob(II)alamin cofactor (*15*). Electron transfer from flavodoxin hydroquinone to four-coordinate cob(II)alamin in the Asp757Glu mutant is nearly equipotential ($\Delta E_m = -4$ mV). For these simulations, the midpoint potential used for the four-coordinate wild-type cob(II)alamin/cob(I)alamin couple is assumed to be the same as the experimentally determined potential for the Asp757Glu enzyme [$E_m = -436$ mV (*16*)]. The observed rate constant for this step is 130 s^{-1} in both wild-type and mutant enzymes; forward and reverse electron transfer rates are calculated assuming $k_{obs} = k_2 + k_{-2}$ and $k_2/k_{-2} = 10^{(-\Delta E_m/59.2)}$. Transfer of the methyl group from AdoMet to the cobalt is irreversible and proceeds with a rate constant of 25 s^{-1}. Dissociation of flavodoxin semiquinone, AdoHcy, and a proton is accompanied by recoordination of His759 to the cobalt. Six-coordinate methylcobalamin enzyme is formed with an observed rate constant of 10 s^{-1}.

formation of six-coordinate methylcobalamin enzyme is calculated by subtracting spectra recorded at 600 and 100 ms (Figure 7B, squares); this spectrum is modeled to conversion of 2.4 μM cob(I)alamin enzyme and 2 μM five-coordinate methylcobalamin enzyme to 4.4 μM six-coordinate methylcobalamin enzyme (solid curve). In each case, the dashed curve represents a calculated spectrum assuming cob(I)alamin enzyme is converted directly to six-coordinate methylcobalamin enzyme. In this experiment, it is apparent that an accurate fit of the kinetic and spectral data is only possible if one assumes that five-coordinate methylcobalamin enzyme is formed as an intermediate following transfer of a methyl group from AdoMet to cob(I)alamin enzyme.

DISCUSSION

Methionine biosynthesis involves transfer of a methyl group from CH_3-H_4folate to homocysteine; both are relatively unreactive substrates at neutral pH. Catalysis is achieved by the cobalamin-dependent methionine synthase in part by using cob(I)alamin as a highly reactive nucleophile toward CH_3-H_4folate. However, cob(I)alamin is a potent reductant, and this catalytic scheme requires that the enzyme either stabilize and protect cob(I)alamin during catalysis or develop a strategy for regenerating cob(I)alamin following inadvertent oxidation. In a strictly anaerobic environment such as is found in methanogenic and acetogenic bacteria, Co^I corrinoids may be relatively stable (*27*). In adapting to an aerobic environment where oxidation to inactive cob(II)alamin is a more common event, *E. coli* has evolved a system that regenerates methylcobalamin enzyme, using flavodoxin as electron donor and AdoMet as methyl donor. Human methionine synthase is reactivated in a similar manner, using reducing equivalents generated by a protein that incorporates flavodoxin- and flavodoxin reductase-like components in a single polypeptide chain (*28*).

The activation system in methionine synthase must circumvent a highly unfavorable redox potential for transfer of electrons to cob(II)alamin. The intracellular redox potential of *E. coli* during aerobic growth is controlled by the NADPH/$NADP^+$ ratio, which is $\approx$1 (*29*), establishing an effective potential of -330 mV (*30*). This potential is much higher than that for free cob(I)alamin/cob(II)alamin, which is -610 mV (*31*). The interactions of methionine synthase with bound cobalamin act to raise the potential of the cob(I)alamin/cob(II)alamin couple to -490 mV (*16*). In principle, conversion of five-coordinate to four-coordinate cob(II)alamin would be expected to further raise the midpoint potential for reduction of cob(II)alamin (*31*). Coupling reduction to irreversible methyl transfer from the reactive methyl donor, AdoMet, provides a large free energy decrease to drive the overall reaction (*10*). Thus, even under aerobic conditions, irreversible methyl transfer from AdoMet is able to trap the small amount of cob(I)alamin produced and eventually return all of the enzyme to the active methylcobalamin form.

To facilitate reduction of cob(II)alamin enzyme, the bound five-coordinate cob(II)alamin prosthetic group is destabilized relative to the free cofactor. At neutral pH, the free cofactor exists in an equilibrium between five- and four-coordinate cob(II)alamin that strongly favors the five-coordinate species [$K_{eq} = 62$ (*31*)], while the enzyme-bound cofactor is $\sim$10$-$15% four-coordinate [$K_{eq} \approx 5.5-9$ (*21*)]. Flavodoxin binds to the cob(II)alamin enzyme, and this interaction further stabilizes the four-coordinate cob(II)alamin conformation, as assessed by EPR and UV/visible spectroscopy (*15*). Measurements of the rate of conversion of five-coordinate to four-coordinate cob(II)alamin upon binding flavodoxin to methionine synthase, described in this paper (Figure 4), demonstrate that the conversion is slow ($k_{obs} \approx 0.4$ s^{-1}). In fact, the rate of four-coordinate cob(II)alamin formation is

comparable to the overall rate of reductive methylation catalyzed by AdoMet and flavodoxin hydroquinone, indicating that this conversion is the rate-limiting step in reductive methylation.

Mutation of Asp757 to glutamate stabilizes four-coordinate cob(II)alamin, bypassing this rate-limiting conformational change and allowing observation of subsequent intermediates in reductive methylation. When Asp757Glu cob(II)alamin enzyme reacts with AdoMet and flavodoxin hydroquinone, cob(I)alamin enzyme forms rapidly ($k_{obs} = 130$ s^{-1}, Figure 6A−C). These experiments with the Asp757Glu mutant enzyme provide the first conclusive spectral evidence that the immediate product of electron transfer is the reduced cob(I)alamin cofactor. Since the difference in midpoint potential between the Asp757Glu cob(I)alamin/cob(II)alamin couple and the flavodoxin hydroquinone/semiquinone couple is known ($\Delta E_{m7} = -4$ mV), and if we assume that complex formation with flavodoxin alters neither redox potential, we can calculate the forward and reverse electron transfer rates as 70 and 60 s^{-1} (Figure 8, assuming $k_{obs} = k_f + k_r$).

The spectral changes observed during this fast electron transfer step (Figure 6C, upper panel) are accurately modeled if we assume that only the ∼70% four-coordinate cob(II)alamin enzyme is reduced by flavodoxin in this phase. The remaining five-coordinate Asp757Glu cob(II)alamin enzyme is methylated at a much slower rate ($k_{obs} \approx 0.5$ s^{-1}, data not shown); presumably this rate is limited by the conversion of five-coordinate to four-coordinate cob(II)alamin enzyme. Either the five-coordinate cob(II)alamin enzyme does not bind flavodoxin productively or the cob(I)alamin/cob(II)alamin couple is too low for effective reduction by flavodoxin. Further experiments will be required to distinguish these possibilities.

In modeling the data for the wild-type enzyme shown in Figure 4, we have assumed the same midpoint potential for reduction of the four-coordinate wild-type enzyme as for the Asp757Glu mutant protein ($E_{m7} = -436$ mV, $\Delta E_m = -4$ mV). However, attempts to measure the midpoint potential of the wild-type methionine synthase in the presence of a 20-fold excess of flavodoxin hydroquinone (300 μM) yielded a value of −510 mV [$\Delta E_m = +60$ mV (*15*)]. Due to uncertainties in our estimates of the initial amount of wild-type four-coordinate cob(II)alamin enzyme and in the transient amount of cob(I)alamin formed [the kinetic phase associated with cob(I)alamin formation overlaps with that for methylcobalamin formation, as shown in Figure 4], we are not able to estimate ΔE_m for the wild-type enzyme accurately from our data and can accommodate a range of values from −40 to +40 mV. The forward and reverse electron transfer rates associated with reduction of wild-type enzyme, calculated explicitly from k_{obs} and ΔE_m for the Asp757Glu mutant enzyme in Figure 8, could likewise encompass a relatively large range of values for the wild-type enzyme: $k_2 = 20-110$ s^{-1} and $k_{-2} = 110-20$ s^{-1}. Thus, our estimates of the ΔE_m values and rates for electron transfer in the wild-type methionine synthase:flavodoxin complex should be regarded as tentative.

The Asp757Glu cob(I)alamin enzyme is rapidly methylated by AdoMet (Figure 6A). The resulting spectral changes (Figure 6C) are modeled most accurately assuming the enzyme initially forms a five-coordinate methylcobalamin enzyme ($k_3 = 25$ s^{-1}) which then converts to six-coordinate methylcobalamin enzyme ($k_4 = 10$ s^{-1}, Figure 8). Chemical reduction of wild-type enzyme allows direct observation of the methyl transfer steps without interference from spectral changes due to electron transfer (Figure 7). When wild-type cob(I)alamin enzyme reacts with AdoMet, the initial spectral changes suggest disappearance of cob(I)alamin and formation of a five-coordinate methylcobalamin enzyme species, similar to the His759Gly mutant enzyme, with an absorption maximum at 450 nm (*21*). This five-coordinate methylcobalamin enzyme is then converted to six-coordinate methylcobalamin enzyme (Figure 7), in a kinetic step that is presumably also associated with flavodoxin dissociation and conversion to the active enzyme conformation involved in primary turnover (*22*). Since five-coordinate methylcobalamin enzyme is not a significant intermediate following methylation of wild-type cob(I)alamin enzyme by CH_3-H_4-folate, even during turnover of Asp757Glu mutant enzyme, formation of a bond between His759 and the cobalt during the catalytic cycle must be inherently faster than methyl transfer, which proceeds with a $k_{obs} \approx 180$ s^{-1} (*9*). Thus, our ability to detect five-coordinate methylcobalamin during reactivation, but not during the catalytic cycle, appears to rest on the coupling of histidine reassociation to a slow conformational change.

We have used several strategies to populate intermediates in reductive methylation in order to visualize these transient enzyme states, including chemical reduction of flavodoxin and cob(II)alamin enzyme, as well as mutation of Asp757 and His759. It is perhaps worthwhile to consider how the details of the kinetic mechanism might differ during aerobic growth of *E. coli*. Under these conditions, $E_{cell} \approx -330$ mV (*17*, *30*), and the predominant oxidation state of flavodoxin bound to methionine synthase is the semiquinone form. Since the flavodoxin semiquinone/oxidized couple has a much higher midpoint potential ($E_{m7} = -260$ mV) than the cob(I)alamin/cob(II)alamin couple, the driving force for electron transfer is low, and therefore the equilibrium concentration of cob(I)alamin and the rate of electron transfer will be significantly decreased. Under aerobic physiological conditions, the rate of reductive methylation is predicted to be primarily limited by the population of cob(I)alamin that can be generated by electron transfer from bound flavodoxin semiquinone. Optimal rates of reductive methylation are achieved under anaerobic conditions where flavodoxin hydroquinone serves as electron donor.

Among the known vitamin B_{12}-dependent enzymes, methionine synthase is unique in its ability to catalyze its own reactivation. To do so requires the selective use of flavodoxin and AdoMet as substrates with oxidized enzyme, without allowing these substrates to interfere in the primary reactions of methionine biosynthesis. Methionine synthase appears to maintain a strict separation between conformations involved in primary turnover and reductive methylation (*22*). The manner in which the enzyme is able to detect the oxidation state of the cobalamin cofactor and to permit or deny conformational interconversion remains one of the more mysterious aspects of this enzyme.

ACKNOWLEDGMENT

We thank Professor David Ballou (University of Michigan) for the use of his stopped-flow spectrophotometer.

REFERENCES

1. Magnum, J. H., and Scrimgeour, K. G. (1962) *Fed. Proc., Fed. Am. Soc. Exp. Biol. 21*, 242.
2. Foster, M. A., Dilworth, M. J., and Woods, D. D. (1964) *Nature 201*, 39−42.
3. Taylor, R. T., and Weissbach, H. (1968) *Arch. Biochem. Biophys. 123*, 109−126.
4. Taylor, R. T., and Weissbach, H. (1969) *Arch. Biochem. Biophys. 129*, 728−744.
5. Guest, J. R., and Woods, D. D. (1960) *Biochem. J. 77*, 422.
6. Hatch, F. T., Larabee, A. R., Cathou, R. E., and Buchanan, J. M. (1961) *J. Biol. Chem. 236*, 1095.
7. Fujii, K., and Huennekens, F. M. (1974) *J. Biol. Chem. 249*, 6745−6753.
8. Taylor, R., and Hanna, M. (1970) *Arch. Biochem. Biophys. 137*, 453−459.
9. Banerjee, R. V., Frasca, V., Ballou, D. P., and Matthews, R. G. (1990) *Biochemistry 29*, 11101−11109.
10. Banerjee, R. V., Harder, S. R., Ragsdale, S. W., and Matthews, R. G. (1990) *Biochemistry 29*, 1129−1135.
11. Fujii, K., Galivan, J. H., and Huennekens, F. M. (1977) *Arch. Biochem. Biophys. 178*, 662−670.
12. Fujii, K., and Huennekens, F. M. (1979) in *Biochemical Aspects of Nutrition* (Yagi, K., Ed.) pp 173−183, Japan Scientific Societies Press, Tokyo.
13. Osborne, C., Chen, L.-M., and Matthews, R. G. (1991) *J. Bacteriol. 173*, 1729−1737.
14. Bianchi, V., Eliasson, R., Fontecave, M., Mulliez, E., Hoover, D. M., Matthews, R. G., and Reichard, P. (1993) *Biochem. Biophys. Res. Commun. 197*, 792−797.
15. Hoover, D. M., Jarrett, J. T., Sands, R. H., Dunham, W. R., Ludwig, M. L., and Matthews, R. G. (1997) *Biochemistry 36*, 127−138.
16. Jarrett, J. T., Choi, C. Y., and Matthews, R. G. (1997) *Biochemistry 36*, 15739−15748.
17. Dunlap, R. B., Harding, N. G. L., and Huennekens, F. M. (1971) *Biochemistry 10*, 88−97.
18. Massey, V., and Hemmerich, P. (1978) *Biochemistry 17*, 9−17.
19. Vetter, J. H., and Knappe, J. (1971) *Z. Physiol. Chem. 352*, 433−446.
20. Drennan, C. L., Huang, S., Drummond, J. T., Matthews, R. G., and Ludwig, M. L. (1994) *Science 266*, 1669−1674.
21. Jarrett, J. T., Amaratunga, M., Drennan, C. L., Sands, R. H., Scholten, J. D., Ludwig, M. L., and Matthews, R. G. (1996) *Biochemistry 35*, 2464−2475.
22. Jarrett, J. T., Huang, S., and Matthews, R. G. (1998) *Biochemistry 37*, 5372−5382.
23. Amaratunga, M., Fluhr, K., Jarrett, J. T., Drennan, C. L., Ludwig, M. L., Matthews, R. G., and Scholten, J. D. (1996) *Biochemistry 35*, 2453−2463.
24. Jarrett, J. T., Goulding, C., Fluhr, K., Huang, S., and Matthews, R. G. (1997) *Methods Enzymol. 281*, 196−213.
25. Hoover, D. M., and Ludwig, M. L. (1997) *Protein Sci. 6*, 2525−2537.
26. Zehnder, A. J., and Wuhrmann, K. (1976) *Science 194*, 1165−1166.
27. Matthews, R. G., Banerjee, R. V., and Ragsdale, S. W. (1990) *BioFactors 2*, 147−152.
28. Leclerc, D., Wilson, A., Dumas, R., Gafuik, C., Song, D., Watkins, D., Heng, H. H. Q., Rommens, J. M., Scherer, S. W., Rosenblatt, D. S., and Gravel, R. A. (1998) *Proc. Natl. Acad. Sci. U.S.A. 95*, 3059−3064.
29. Anderson, K. B., and von Meyenberg, K. (1977) *J. Biol. Chem. 252*, 4151−4156.
30. Clark, W. M. (1960) *Oxidation−Reduction Potentials of Organic Systems*, Waverly Press, Baltimore.
31. Lexa, D., and Savéant, J. M. (1976) *J. Am. Chem. Soc. 98*, 2652−2658.

BI9808565